

# AN IRIS DIAPHRAGM BEAM DETECTOR FOR HALO OR PROFILE MEASUREMENTS\*

A. Liu<sup>†</sup>, on behalf of the project, Euclid Techlabs, LLC, Bolingbrook, U.S.A.

## Abstract

Non-Gaussian beam distributions around the Gaussian core can be formed in an accelerator in both the transverse and longitudinal directions. Since there are no clearly defined criteria to distinguish the halo from the core, the measurement of the halo structure without affecting the core is challenging. Both destructive and non-destructive techniques have been developed and tested at various accelerator facilities. Most of these techniques require complex and expensive setups, like in a gas sheet monitor, or a digital micromirror array. In this paper, a novel device that adopts an iris diaphragm structure for transverse beam halo measurement is presented. The iris diaphragm detector can also work as an adjustable collimator. It also has advantages such as high-portability, cost-effectiveness, high-configurability and more. A proof-of-principle version-alpha of the detector has been successfully tested at the ACT beamline of AWA at ANL. The design of a version-beta is also discussed in the paper.

## INTRODUCTION

There are multiple mechanisms to form a beam halo structure. It can be from the dark current in an accelerator, or from beam scattering with residual gas molecules in the vacuum chambers, and so forth. Although the halo formation mechanisms may differ, the hazards it presents to the machine operation and the users (such as those light source users) are common concerns for the facilities. The halo beam can deposit overwhelming energy and generate radiations that impacts the detector lifetime or even destroy the detector in a short time window.

Researchers have been exploiting methods to measure the beam halo, using non-destructive, partially-destructive, or completely-destructive techniques. Among the non-destructive methods, the usage of synchrotron radiation light with a digital micromirror array [1, 2], gas sheets monitor are novel techniques that are actively investigated. Among the destructive methods, the use of a Wire Scanner (WS) [3] is one of the most commonly adopted. Most of the methods, however, require complex and expensive setups.

Inspired by the structure of an iris diaphragm for a camera lens, Euclid Techlabs, LLC started developing an iris diaphragm beam transverse halo or profile detector (referred to as iris detector hereafter) from Feb, 2019. The iris detector uses metal iris blades to stop and absorb the charged particles, for which the current is extracted from each blade as an independent signal. The iris closes to intercept the

beam, and opens to stop intercepting. Each blade is insulated from the others and generates an independent signal. The pulsed current signals are transported to outside the vacuum through an SMA feedthrough port mounted onto a CF flange. The open-and-close motion of the iris blades can be controlled and driven by a linear actuator. The whole apparatus can be contained in a six-way 6" CF cross. It has the advantages to be *cost-efficient*, *highly-configurable*, *dual-purposed*, and *linearly-responsive*. Furthermore, it can be designed to work *both as a transverse profile detector, and as a movable collimator*, simultaneously.

## PROOF-OF-PRINCIPLE VERSION-ALPHA

The version-alpha of the iris detector (referred to as version-alpha hereafter) is a prototype to demonstrate the following proofs-of-principle:

- Pulsed current signals can be generated and sent from an iris blade, which works as a beam collector when being bombarded by an electron beam, through the SMA ports and be read by an oscilloscope.
- When the beam energy is high, or when the stopping power of the iris blade is small, such that a fraction of the charged particles penetrate the blades, the blades can work properly with the partial beam current deposited onto the blades.
- The signal isolation between iris blades can be achieved by using ceramic plates, on which the blades translate in opposition, while the signal on each blade is independent of the other.

The 3D design of the version-alpha is shown in Fig. 1. A metallic holder that has multiple slots for holding iris blades of different materials and different thickness is mounted to a UHV-compatible linear actuator on the top. A 45°-angle YaG screen is attached to an adapter, which is then mounted to the bottom of the holder. The holder and YaG adapter are conductive with each other, and a coax cable is used to connect the holder and one of the SMA ports (upper brown line in the figure). A metallic contactor with two vertical pillars is mounted on but insulated from a rotary feedthrough on the bottom. Ceramic sheets can be mounted on the side faces of the pillars. The purpose of the design is to touch the YaG adapter from different faces, thus providing either a metal-to-metal contact, or a metal-ceramic-metal contact to test ceramic insulation. Another coax cable connects the contactor and the other SMA port (lower brown line). Both top and bottom signals are insulated from either of the feedthrough shafts, thus only go through the SMA ports. The cables are guided by a structure, which is mounted on the 6" to 2.75" zero-length reducer for the SMA ports. The structure guides the cables to slide through the two holes in

\* Work supported by the SBIR program of the U.S. Department of Energy, under grant DE-SC0019538, PI: A. Liu

<sup>†</sup> a.liu@euclidtechlabs.com

a controlled manner, instead of interfering with the beam path, or with the linear and rotary feedthrough motions.

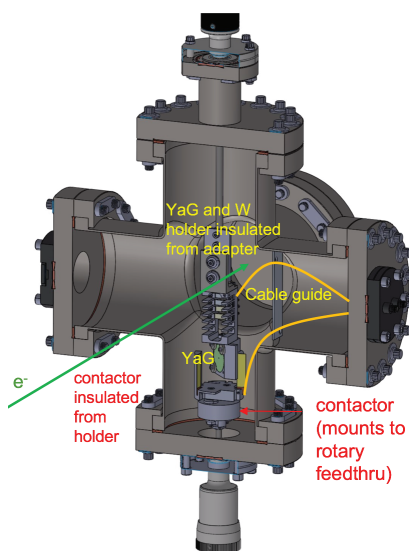


Figure 1: The proof-of-principle design of an iris detector version-alpha. The green arrow shows the electron beam direction of motion. The metallic iris blade holder (slotted structure hung from top) and the metallic contactor (with two pillars, mounted on the bottom) are both insulated from the linear (top) and rotary (bottom) feedthroughs using ceramic structures. The brown lines are the coax cables.

The top four iris blade holder slots were filled with W or Al blades to give different stopping power. The topmost slot has the least stopping power provided by a 0.040"-thick Al blade, while the 4<sup>th</sup> slot has the most stopping power given by a 0.125"-thick W blade. The Geant4 [4] simulations of a 1.5 MeV  $e^-$  beam on the two different blades are shown in Fig. 2. The beam is mostly absorbed or back-scattered by the W blade, while a large fraction of it penetrates the Al blade and some are absorbed.

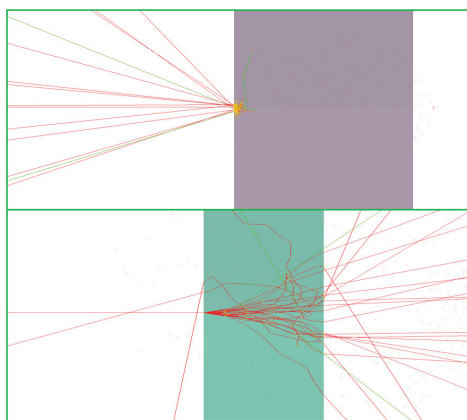


Figure 2: The Geant4 simulations of the  $e^-$  beam interactions with matters for 0.125"-thick Tungsten and 0.040"-thick Al. The red traces are  $e^-$  and the green ones are photons.

## EXPERIMENTS AT AWA

The fabricated apparatus was sent to the Argonne Wakefield Accelerator (AWA) facility at Argonne National Laboratory (ANL) for experimental tests. All the parts were thoroughly cleaned following a procedure set by the Advanced Photon Source (APS) at ANL to meet the stringent vacuum requirement at AWA ( $< 10^{-8}$  Torr). The cleaned parts were then assembled together by Euclid and AWA personnel. The assembly was installed at the downstream end of the ACT [5] beamline of AWA. The schematic drawing of the ACT beamline and the installed version-alpha is shown in Fig. 3. There is an ICT before the version-alpha for measuring the total beam current delivered to the apparatus.

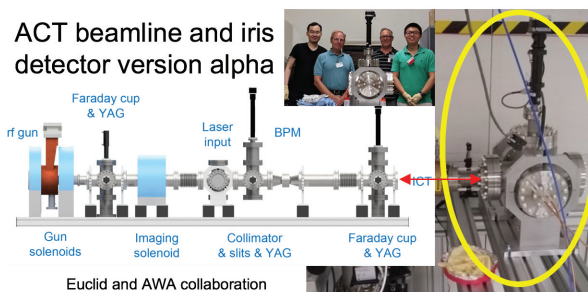


Figure 3: The schematic drawing of the ACT beamline at AWA of ANL, and the installed version-alpha at the end of ACT.

Due to the planned laser upgrade at AWA, the experiments were compressed to two days. Nevertheless, all the planned tests were completed in the short time window. The version-alpha experiment was the *first time* that the ACT beam is used in a physics experiment other than testing the cathode performance itself. Since the ACT beamline was not originally designed as a user facility, which guarantees a stable beam delivery, the electron beam had a noticeable transverse jitter, and the size could sometimes be as big as that of the YaG screen. Moreover, because of the pending laser upgrade, the beam intensity and size jitter was much more drastic than normally seen in a daily operation condition. Nevertheless, the signal from the blade holder was much stronger than that from the ICT. The preliminary experimental data analysis results are given below (see Fig. 4).

### Noisy Raw Signal Data and LP Filtering

There can be multiple sources of noises in the setup. As the beam size was bigger than the blades, the escaped primary electrons and scattered electrons from the surface may interfere with the coax cable and generate high-frequency noises. Electrons that are absorbed by the six-way cross can also generate high-frequency noise. However, these noises are easy to identify and filter out. A low-pass (LP) filter was applied to the raw signal to get the correct pulsed negative current amplitude. Figure 5 shows the raw, a high-pass (HP) filtered, and a LP filtered signal from the blade holder and the contactor, when the beam is fully intercepted by the YaG

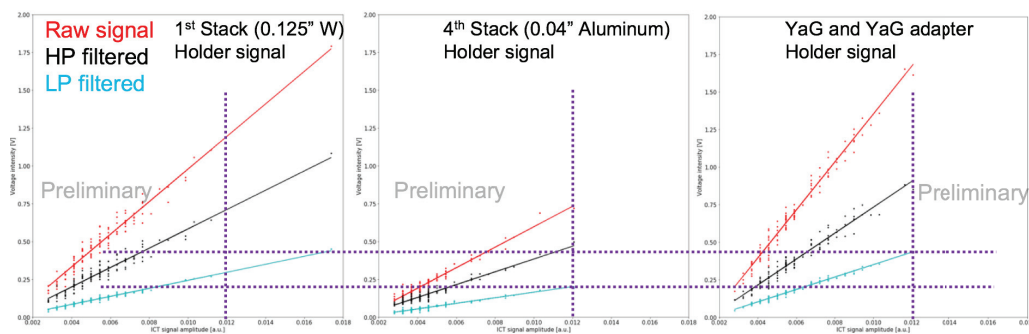


Figure 4: Comparison of signal strengths from the three beam interception configurations.

screen and adapter. The bottom contactor did not contact the top blade holder. Due to impedance mismatch in the connection to the SMA port (notice that it was not designed to have a  $50 \Omega$  impedance, which is not required to have a correct signal response), the strongest negative peak was followed by a decaying reflection pattern. It also shows the holder-coax-SMA connection has an RC circuit structure, in which the picosecond (ps)-scale pulse was elongated.

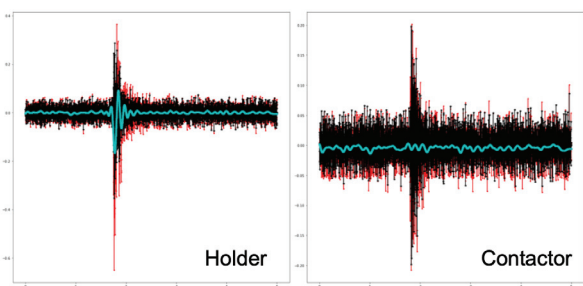


Figure 5: The raw, HP-filtered and LP-filtered signals from the top blade holder and bottom contactor. Red: raw signal, black: HP-filtered signal, cyan: LP-filtered signal.

### Beam Current from Different Blades

The electron beam was intercepted in three ways as comparisons: by a 0.125" W blade, a 0.040" Al blade, and the YaG and its adapter. The YaG adapter is a few centimeters thick in the beam direction, which is sufficient to fully absorb the beam. The pulsed signal strength versus the ICT signal amplitude measured at the same beamline configuration but at different laser-synced pulses is shown in Fig. 4. The YaG adapter is the most efficient element in absorbing the charges, because of the back scattering at the surface of the high-Z Tungsten blade, and the beam penetration in the Al blade. Another configuration, which is not shown in the figure is intercepting the beam using a thinner (0.040"-thick) Tungsten blade. The signal strength was almost identical to that from the 0.125"-thick blade, because approximately all electron absorption occurred prior to 0.040".

### VERSION-BETA DESIGN

After the successful tests of the version-alpha, Euclid is working on the design and fabrications of the iris detector

version-beta. In this version, four blades are used as the iris, which are oriented in the four quadrants in the X-Y plane. The SolidWorks design schematics are shown in Fig. 6. The plan is to test the version-beta at ACT by early November, 2019.

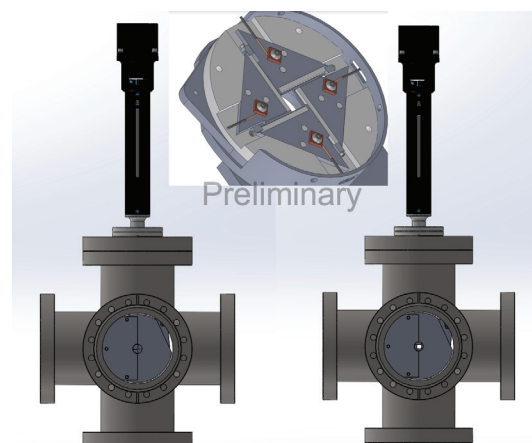


Figure 6: The SolidWorks design schematics of the version-beta. The close and open conditions (left and right), and the ceramic holder for iris blades (middle) are shown.

### CONCLUSION AND FUTURE WORK

The iris diaphragm beam halo or profile detector is a novel, cost-effective and dual-purpose (collimator) charge current detector. The proof-of-principle version-alpha was recently successfully tested using the 1 MeV  $e^-$  beam at the ACT beamline of AWA at ANL. The experimental results indicate the theoretical bases of the apparatus are all intact. A version-beta is being designed and fabricated, which is planned to be tested at ACT by early November of 2019.

### ACKNOWLEDGEMENTS

The author would like to thank the whole project group at Euclid, especially Scott Ross, Chunguang Jing, Yubin Zhao, and Alexei Kanareykin, for their discussions and support. The author also thanks the AWA group for the invaluable support for the experiments, especially Jiahang Shao and Eric Wisniewski.

Content from this work may be used under the terms of the CC BY 3.0 licence (© 2019). Any distribution of this work must maintain attribution to the author(s), title of the work, publisher, and DOI

## REFERENCES

- [1] H. Zhang, R. Fiorito, A. G. Shkvarunets, R. Kishek, and C. P. Welsch, “Beam Halo Imaging with a Digital Optical Mask,” H. Zhang, et al., *Phys. Rev. Accel. and Beams*, vol. 15, no. 7, p. 072803, Jul. 2012. doi:10.1103/PhysRevSTAB.15.072803
- [2] C. P. Welsch, T. Cybulski, A. Jeff, V. Tzoganis, and H. D. Zhang, “Non-invasive Beam Profile Monitoring”, in *Proc. IPAC’15*, Richmond, VA, USA, May 2015, pp. 537–539. doi:10.18429/JACoW-IPAC2015-MOPMA005
- [3] S. Liu *et al.*, “First Beam Halo Measurements Using Wire Scanners at the European XFEL”, in *Proc. FEL’17*, Santa Fe, NM, USA, Aug. 2017, pp. 255–258. doi:10.18429/JACoW-FEL2017-TUP003
- [4] GEANT4, <https://geant4.web.cern.ch/>
- [5] J. Shao *et al.*, “In situ Observation of Dark Current Emission in a High Gradient RF Photocathode Gun,” *Phys. Rev. Lett.*, vol. 117, no. 8, p. 084801, Aug. 2016. doi:10.1103/PhysRevLett.117.084801